

# *Foxa2* mediates critical functions of prechordal plate in patterning and morphogenesis and is cell autonomously required for early ventral endoderm morphogenesis

Zachary Harrelson<sup>1</sup>, Klaus H. Kaestner<sup>2</sup> and Sylvia M. Evans<sup>1,3,\*</sup>

<sup>1</sup>Skaggs School of Pharmacy and Pharmaceutical Sciences, University of California San Diego, 9500 Gilman Drive MC0613C, La Jolla, CA 92093, USA

<sup>2</sup>Department of Genetics, University of Pennsylvania, 752b Clinical Research Building, 415 Curie Boulevard, Philadelphia, PA 19104, USA

<sup>3</sup>School of Medicine, University of California San Diego, 9500 Gilman Drive MC0613C, La Jolla, CA 92093, USA

\*Author for correspondence (syevans@ucsd.edu)

*Biology Open* 1, 173–181  
doi: 10.1242/bio.2012040

## Summary

Axial mesendoderm is comprised of prechordal plate and notochord. Lack of a suitable Cre driver has hampered the ability to genetically dissect the requirement for each of these components, or genes expressed within them, to anterior patterning. Here, we have utilized *Isl1-Cre* to investigate roles of the winged helix transcription factor *Foxa2* specifically in prechordal plate and ventral endoderm. *Foxa2*<sup>loxP/loxP</sup>; *Isl1-Cre* mutants died at 13.5 dpc, exhibiting aberrations in anterior neural tube and forebrain patterning, and in ventral foregut morphogenesis and cardiac fusion. Molecular analysis of *Foxa2*<sup>loxP/loxP</sup>; *Isl1-Cre* mutants indicated that *Foxa2* is required in *Isl1* lineages for expression of notochord and dorsal foregut endoderm markers, *Shh*, *Brachyury*, and *Hlx9*. Our results support a requirement for *Foxa2* in

prechordal plate for notochord morphogenesis, axial patterning, and patterning of dorsal foregut endoderm. Loss of *Foxa2* in ventral endoderm resulted in reduced expression of *Sox17*, *Gata4*, and *ZO* proteins, accounting at least in part for observed lack of foregut fusion, cardia bifida, and increased apoptosis of ventral endoderm.

© 2012. Published by The Company of Biologists Ltd. This is an Open Access article distributed under the terms of the Creative Commons Attribution Non-Commercial Share Alike License (<http://creativecommons.org/licenses/by-nc-sa/3.0>).

Key words: axial mesendoderm, notochord, *Isl1*, foregut pocket

## Introduction

Axial mesendoderm is a transient midgestation tissue located at the midline of 7.0–8.5 day post coitus (dpc) mouse embryos which is critical for patterning adjacent tissues, including neural ectoderm and paraxial mesoderm (Jessell, 2000; Wilson and Maden, 2005; Lee and Anderson, 2008). Axial mesendoderm is derived from anterior regions of primitive streak during gastrulation including the node organizer, is initially contiguous with endodermal epithelium, and is anatomically distinct due to its direct apposition with overlying neural groove ectoderm (Jurand, 1974; Beddington, 1994; Sulik et al., 1994; Kinder et al., 2001; Lewis and Tam, 2006; Yamanaka et al., 2007; Lee and Anderson, 2008).

Axial mesendoderm is comprised of notochordal plate and prechordal plate, the most anterior mesendoderm (Sulik et al., 1994; Yamanaka et al., 2007). Notochordal plate will give rise to notochord and contribute to dorsal foregut endoderm, and prechordal plate will contribute to ventral foregut endoderm, oral endoderm, and ventral cranial mesoderm (Couly et al., 1992). Tissue ablation studies have demonstrated that prechordal plate reinforces forebrain induction and regulates other aspects of anterior development (Shimamura and Rubenstein, 1997; Camus et al., 2000). Additionally, defects in anterior embryonic

patterning have been associated with disruption of prechordal plate markers (Ang and Rossant, 1994; Weinstein et al., 1994; Filosa et al., 1997; Bachiller et al., 2000; Petryk et al., 2004; Nishioka et al., 2005; Warr et al., 2008). Attribution of tissue specific roles of genes expressed in prechordal plate in notochord development, however, has been limited by the lack of a prechordal plate-specific Cre line that is not active in other axial mesendodermal regions.

The forkhead transcription factor *Foxa2* is expressed in critical signaling centers during development, including node, notochord, and prechordal plate, and is also expressed in both extraembryonic and embryonic endoderm. Global knockout of *Foxa2* has revealed critical roles in embryonic patterning and a requirement for endoderm formation (Ang and Rossant, 1994; Weinstein et al., 1994; Dufort et al., 1998). Conditional *Foxa2* deletion utilizing an endodermal-specific *Foxa3-Cre* line, however, did not result in defects in gut formation, perhaps owing to persistence of *Foxa2* protein in mutant foregut endoderm at 9.5 dpc (Lee et al., 2005). Thus far, roles for *Foxa2* in prechordal plate, or in early ventral endoderm, have not been investigated.

Dorsal and ventral foregut endoderm have unique embryonic origins, with distinct timing of emergence from the primitive

streak and divergent migratory pathways that converge to comprise the entire foregut endoderm (Tremblay and Zaret, 2005; Tam et al., 2007). Gut tube formation begins in the anterior embryo at early to late head fold stages (EHF-LHF, ~8.0–8.25 dpc) when an initially flat sheet of endodermal epithelium is transformed into a pocket structure. Ventral midline of the foregut is a discrete population derived from prechordal plate (Kirby et al., 2003; Franklin et al., 2008; Aoto et al., 2009). The foregut pocket remains open anterior to the site of fusion, termed the anterior intestinal portal.

To investigate tissue-specific roles for *Foxa2* in prechordal plate and ventral foregut endoderm, we have ablated *Foxa2* utilizing *Isl1-Cre* (Sund et al., 2000; Yang et al., 2006). Use of *Isl1-Cre* has allowed us to genetically isolate prechordal plate from posterior axial mesendoderm to address patterning by axial mesendoderm, and our results reveal a requirement for prechordal plate in development of notochord and dorsal foregut endoderm, both derivatives of notochordal plate. Our data also demonstrate a cell autonomous role for *Foxa2* in ventral foregut endoderm for endoderm specification and foregut morphogenesis.

## Results

*Isl1-Cre* lineages overlap with *Foxa2* in prechordal plate, ventral foregut and yolk sac endoderm

To investigate overlap between *Isl1-Cre* and *Foxa2* expression, *Isl1-Cre; Rosa<sup>+26R-lacZ</sup>* embryos were analyzed beginning at early headfold (EHF) stages. Whole mount X-gal staining of EHF *Isl1-Cre; Rosa<sup>+26R</sup>* embryos demonstrated low levels of  $\beta$ -galactosidase staining in the allantois. At these stages,  $\beta$ -galactosidase-positive domains were not detected in the embryo proper or in yolk sac endoderm anterior to the emergent head folds (supplementary material Fig. S1). At 3–5 som,  $\beta$ -galactosidase staining was not detected in extraembryonic tissues

outside of the allantois in *Isl1-Cre; Rosa<sup>+26R-lacZ</sup>* embryos (supplementary material Fig. S1). *Isl1-Cre* activity is first evident in embryonic endoderm at 2–3 som (Park et al., 2006). At this stage, histological section analyses demonstrated that *Isl1-Cre*-derived cells were present in prospective ventral foregut caudal to the foregut pocket, and in ventral foregut endoderm extending to the rostral pocket tip (Fig. 1A–F). Rostralmost *Isl1-Cre* labeled cells included prechordal plate as indicated by direct apposition to overlying neural ectoderm, consistent with previous studies demonstrating *Isl1* expression in prechordal plate in chick embryos (Yuan and Schoenwolf, 2000). *Isl1-Cre*-derived cells were also evident in head and heart mesoderm (Tzahor and Evans, 2011), and in yolk sac endoderm underlying the heart.

Examination of *Foxa2* expression by immunohistochemistry demonstrated that *Foxa2* and *Isl1-Cre* overlapped in prechordal plate, foregut endoderm, and yolk sac endoderm underlying cardiogenic mesoderm (Fig. 1G–I). As expected, ablation of *Foxa2* with *Isl1-Cre* resulted in reduction of *Foxa2* expressing cells in overlapping regions including prechordal plate (Fig. 1J), ventral foregut endoderm (Fig. 1K,L), and yolk sac endoderm underlying the heart (Fig. 1J). *Foxa2* expression was also diminished in the midline of the neural groove (Fig. 1J,K), indicating a non-cell autonomous loss of *Foxa2* in this expression domain.

Further analysis confirmed that *Isl1-Cre* lineages did not overlap with *Foxa2* expression in node, notochordal plate or its derivatives, including dorsal foregut endoderm and notochord, or floor plate of the neural tube (Fig. 2).

*Foxa2* is required in *Isl1* lineages for forebrain and anterior embryonic patterning, and for heart and foregut morphogenesis. Previous studies have demonstrated a role for *Foxa2* in axial mesendoderm for forebrain and anterior embryonic patterning. However, owing to lack of suitable Cre drivers, it has been

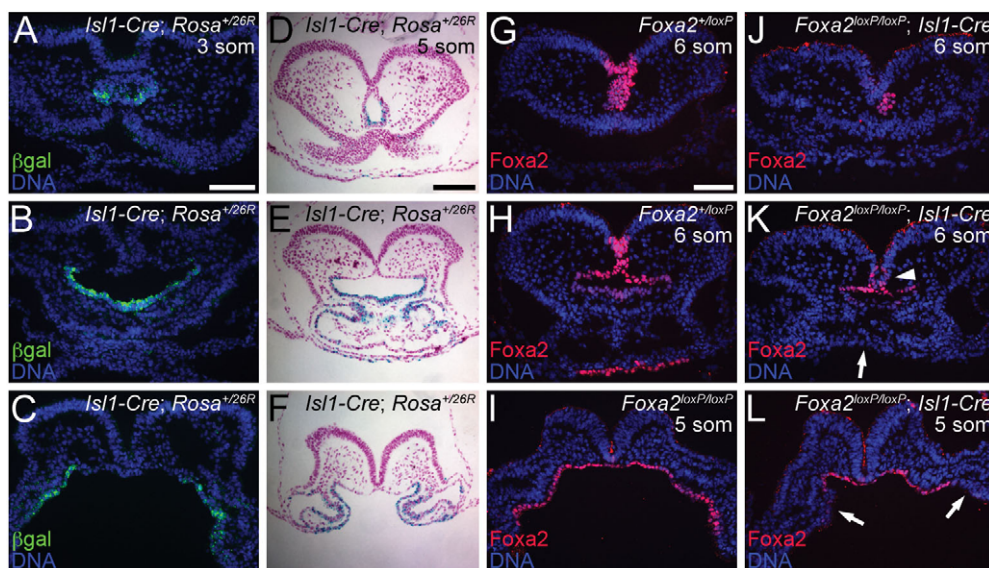


**Fig. 1. *Isl1-Cre* lineages and *Foxa2* expression.** Section analysis of *Isl1-Cre; Rosa26R-lacZ* embryos, immunostaining for  $\beta$ -galactosidase (A–C) or by X-gal staining (D–F), demonstrated *Isl1-Cre* labeling in prechordal plate (A, D), foregut endoderm (B, E, D, F), and yolk sac endoderm underlying the heart (E). Section immunostaining with antibodies to *Foxa2* in control embryos (G–I) demonstrated overlapping expression of *Foxa2* and *Isl1-Cre* lineages in prechordal plate (G), ventral foregut endoderm (H, I), and yolk sac endoderm underlying the heart (H). *Isl1-Cre* lineages were not observed in other sites of *Foxa2* expression, including ectoderm of the neural groove (future floorplate) (G, H), notochord (I), or dorsal endoderm (H). Section immunostaining with antibodies to *Foxa2* in *Foxa2loxP/loxP; Isl1-Cre* stage-matched littermate mutant embryos demonstrated reduction of *Foxa2* expression in prechordal plate (J), ventral foregut (K, L), and yolk sac endoderm (K) (white arrows). *Foxa2* expression was also reduced in the midline of the neural groove (J, K) (white arrowhead).

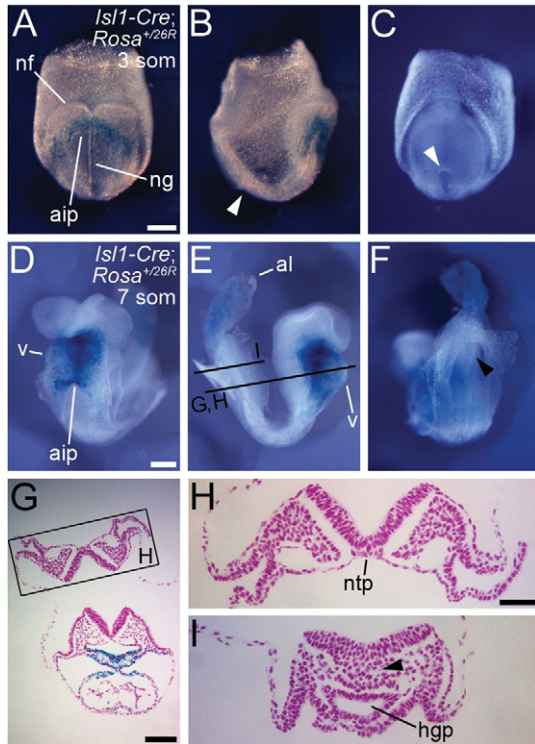


**Fig. 2. *Isl1-Cre* lineages do not include node or notochord, 8.25–8.5 dpc.** (A–C) X-gal-stained *Isl1-Cre; Rosa<sup>+/26R</sup>* embryo, 3 som, anterior (A), right (B), posterior (C) views. *Isl1* lineages did not include node (white arrowheads in B, C). (D–F) X-gal-stained *Isl1-Cre; Rosa<sup>+/26R</sup>* embryo, 7 som, anterior-left (D), right (E), posterior (F) views. *Isl1* lineages did not include notochordal plate (black arrowhead in F). Black lines in E indicate planes of section for G–I. (G) Section through foregut and ventricle of embryo in D. Black box indicates posterior embryo region shown at high magnification in H. (H–I) Sections through posterior embryo regions with (H) notochordal plate (ntp) or (I) hindgut pocket (hgp). Black arrowhead in I marks site of continued gastrulation. Bar in: A is 0.2 mm for A–C; D is 0.2 mm for D–F; G is 0.1 mm; H is 0.05 mm for H–I. aip, anterior intestinal portal; al, allantois; nf, neural fold; ng, neural groove; v, ventricle.

difficult to dissect the requirement for *Foxa2* in prechordal plate from its requirement in other axial patterning tissues. Our analysis of *Isl1-Cre* lineages demonstrated that *Isl1-Cre* would allow us to selectively examine the cell autonomous requirement for *Foxa2* in prechordal plate in forebrain and anterior patterning apart from its requirement in notochord or floorplate. To investigate the potential role of *Foxa2* in tissues which overlapped with those labeled by *Isl1-Cre*, including prechordal plate and foregut endoderm, we utilized *Isl1-Cre* to generate tissue-specific deletion of *Foxa2*.

Heterozygous *Foxa2<sup>+/loxP</sup>; Isl1-Cre* mice were viable, fertile, and displayed no obvious abnormalities. Most homozygous *Foxa2<sup>loxP/loxP</sup>; Isl1-Cre* mutants were dead by 12.5–13.5 dpc ( $n=9/11$ , supplementary material Table S1), were morphologically distinct at 8.5 dpc ( $n=31/41$ ), and displayed a range of phenotypes (supplementary material Table S2; Fig. 3). Mutant embryos displayed defects in anterior patterning, including abnormal head fold morphology, and abnormal neural groove (Fig. 3C,E). Laterality defects were evidenced by reversed or no cardiac looping in some mutants. Lack of foregut closure and cardia bifida were also seen (Fig. 3E, F; supplementary material Fig. S2). Previous studies have demonstrated that defects in endoderm which result in lack of

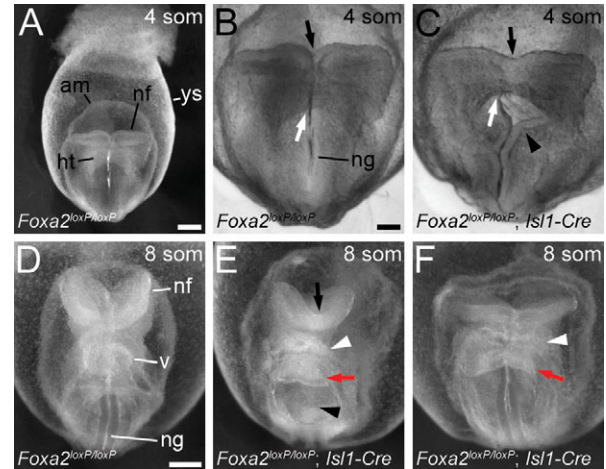


**Fig. 3. Anterior patterning and cardiac defects in *Foxa2<sup>loxP/loxP</sup>; Isl1-Cre* embryos, 8.5 dpc.** (A) 8.5 dpc *Foxa2<sup>loxP/loxP</sup>* embryo, 4 somite pairs (4 som), anterior brightfield view. (B) Close-up view of embryo shown in A. (C) Close-up view of *Foxa2<sup>loxP/loxP</sup>; Isl1-Cre* embryo, 4 som. Black arrows in B–C mark rostral neural groove, white arrows anterior intestinal portal. Black arrowhead in C shows abnormal neural groove. (D–F) 8.5 dpc *Foxa2<sup>loxP/loxP</sup>* (D) and *Foxa2<sup>loxP/loxP</sup>; Isl1-Cre* (E–F) embryos, 8 som, anterior views. Mutant in E lacked neural groove in rostral and trunk regions (black arrows). Abnormal cardiac development is evident in mutant embryos. White arrowheads in E–F mark yolk sac, amnion attachment above or at level of cardiac anlagen (red arrows). Bar in: A is 0.2 mm; B is 0.1 mm for B–C; D is 0.2 mm for D–F. am, amnion; ht, heart; nf, neural fold; ng, neural groove; v, ventricle; ys, yolk sac.

foregut closure can result in cardia bifida (Maretto et al., 2008; Alexander et al., 1999). Holoprocencephaly, a disorder resulting from deficient ventral forebrain patterning (Muenke and Beachy, 2000), was also observed (supplementary material Fig. S1).

To determine whether ectopic *Isl1-Cre* activity contributed to the range of phenotypes observed at 9.5–10.5 dpc, *Foxa2<sup>loxP/loxP</sup>; Isl1-Cre* embryos were generated on a *Rosa<sup>26R-lacZ</sup>* lineage reporter background (Soriano, 1999; Yang et al., 2006). Results showed specific *Isl1-Cre* expression in mutants displaying the full spectrum of abnormalities (supplementary material Fig. S2C–E’).

To investigate whether defects in anterior patterning were separable from defects in foregut closure and cardia bifida, mutants were analyzed for mutual exclusivity of these two broad classes of phenotypes (supplementary material Table S3). Results of this analysis demonstrated that these abnormalities in foregut and cardiac morphogenesis could occur in the absence of defects in anterior patterning, suggesting distinct spatial and/or temporal requirements for *Foxa2* for these two aspects of the *Foxa2<sup>loxP/loxP</sup>; Isl1-Cre* mutant phenotype.

Abnormal development of axial mesendoderm in *Foxa2<sup>loxP/loxP</sup>; Isl1-Cre* mutants is associated with increased apoptosis. Specific defects in anterior patterning and laterality defects as evidenced by reversed or no cardiac looping in *Foxa2<sup>loxP/loxP</sup>; Isl1-Cre* mutants suggested perturbations in axial mesendoderm. In situ hybridization was used to assay axial mesendoderm marker gene expression in 8.0–8.5 dpc *Foxa2<sup>loxP/loxP</sup>; Isl1-Cre* mutants. At these stages, *Gooseoid (Gsc)*, a homeobox transcription factor, is a marker of prechordal plate (Filosa et al., 1997). *Foxa2<sup>loxP/loxP</sup>; Isl1-Cre* mutants exhibited markedly

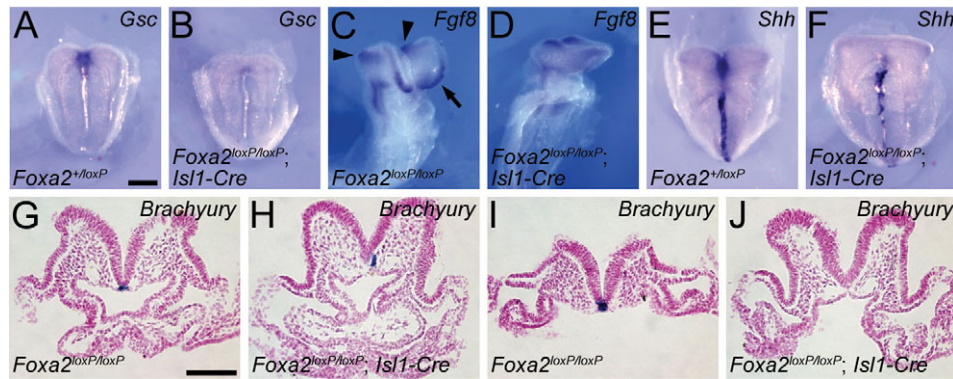


**Fig. 4.** Axial mesendoderm marker gene expression in *Foxa2loxP/loxP; Isl1-Cre* embryos, 8.0–8.5 dpc. (A–B) In situ hybridization (ISH) to detect *Gsc* in *Foxa2+/loxP* (A) and *Foxa2loxP/loxP; Isl1-Cre* (B) embryos, 6 som, anterior views. (C–D) ISH to detect *Fgf8* in *Foxa2loxP/loxP* (C) and *Foxa2loxP/loxP; Isl1-Cre* (D) embryos, 8 som, anterior-right views. Control embryos expressed *Fgf8* in anterior neural ridge (black arrow) and neural ectoderm at midbrain-hindbrain boundary (black arrowheads). (E–F) ISH to detect *Shh* in *Foxa2+/loxP* (E) and *Foxa2loxP/loxP; Isl1-Cre* (F) embryos, 5 som, anterior views. (G–J) Transverse sections after ISH to detect *Brachyury* in *Foxa2loxP/loxP* (G, I) and *Foxa2loxP/loxP; Isl1-Cre* (H, J) embryos, 7 som. (G–H) Sections through foregut with midline heart. (I–J) Sections posterior to the anterior intestinal portal. Bar in: A is 0.2 mm for A–F; G is 0.1 mm for G–J.

reduced *Gsc* expression at E8.0 (6 som) (Fig. 4B). *Fibroblast growth factor 8* (*Fgf8*) marks anterior neural ridge, a signaling center that interacts with prechordal plate to regulate anterior forebrain patterning and expansion (Crossley and Martin, 1995; Shimamura and Rubenstein, 1997). *Fgf8* is also expressed at the midbrain-hindbrain boundary (Fig. 4C). Expression of *Fgf8* in anterior neural ridge was reduced in mutant embryos, while its expression at the midbrain-hindbrain junction was unaffected (Fig. 4D).

*Sonic hedgehog* (*Shh*) is a secreted factor expressed throughout axial mesendoderm which is required for survival of prechordal plate cells and dorsal ventral patterning of the neural tube (Echelard et al., 1993; Chiang et al., 1996; Ding et al., 1998; Aoto et al., 2009). At E8.0, *Shh* mRNA expression was absent in anterior regions of mutant embryos. Trunk regions exhibited patchy expression of *Shh* which did not extend to posterior regions as observed in somite-matched controls (Fig. 4E–F). Immunostaining confirmed that *Shh* protein was also absent from anterior regions of *Foxa2loxP/loxP; Isl1-Cre* mutants, and was abnormally positioned to the left of the midline in more posterior regions (supplementary material Fig. S3).

*Brachyury* is a T-box transcription factor expressed in notochord at 8.5 dpc (Fig. 4G,I). Notochord cells marked by *Brachyury* expression were disorganized and abnormally positioned to the left of the midline in mutant embryos (7 som) (Fig. 4H), while other more anterior and posterior regions showed complete absence of *Brachyury* expression (Fig. 4J).

TUNEL and immunohistochemistry to detect *Brachyury* were used to investigate notochord survival in 8.5 dpc *Foxa2loxP/loxP; Isl1-Cre* mutants. In control littermates, notochord cells were detected in a continuous anterior-posterior domain, and were not associated with apoptosis (Fig. 5A–D). Again, *Brachyury* was absent from the anterior region of mutant embryos (Fig. 5E–F). The most anterior limit of *Brachyury* expression was detected posterior to the anterior intestinal portal and positive cells were again observed to be somewhat disorganized and abnormally positioned leftward of the neural groove (Fig. 5H). In mutant embryos, apoptosis was observed in midline regions rostral to *Brachyury* expression (Fig. 5).

Notochord abnormalities do not correlate with loss of *Foxa2* in ventral endoderm

Our data demonstrated that loss of *Foxa2* in regions which overlap with *Isl1-cre* lineages resulted in defects in notochord formation and morphogenesis. *Isl1-cre* lineages overlap with *Foxa2* in both prechordal plate and ventral foregut endoderm. In individual mutant embryos, we observed loss of notochord

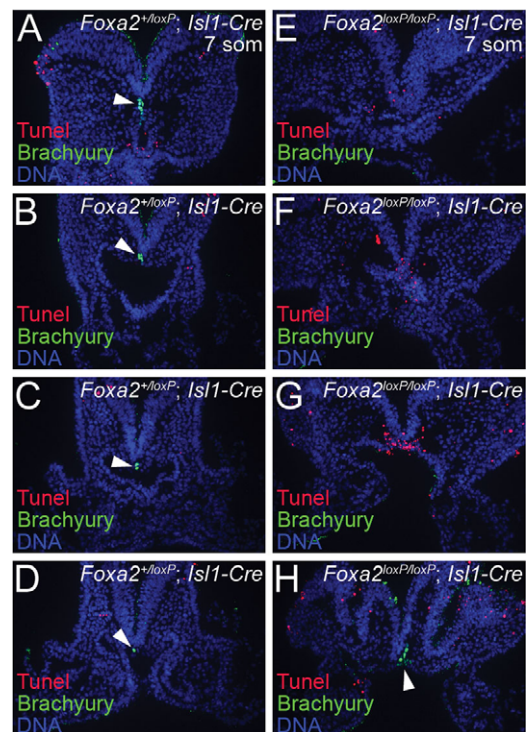


**Fig. 5.** Notochord and apoptosis in *Foxa2loxP/loxP; Isl1-Cre* embryos, 8.5 dpc. TUNEL staining and immunohistochemistry to detect *Brachyury* on transverse section series of *Foxa2+/loxP; Isl1-Cre* (A–D) and *Foxa2loxP/loxP; Isl1-Cre* (E–H) embryos, 7 som. Sections are anterior to posterior (A to D for control, E to H for mutant). White arrowheads (A–D, H) indicate notochord as marked by *Brachyury* expression.

markers even when *Foxa2* was present in ventral foregut endoderm, suggesting that loss of notochord markers is not consequent to loss of *Foxa2* in ventral foregut endoderm (Fig. 6A–H). Notochord defects were scored by absence of a morphologically recognizable notochord structure and lack of characteristic floor plate morphology, lack of *Foxa2* protein expression in neural plate midline, and lack of detectable Brachyury or *Shh* protein expression. *Hlxb9* is expressed in notochord and dorsal endoderm, and was also found to be greatly reduced in both tissues in these mutants (Fig. 6F). In other mutants, expression of axial tissue and dorsal foregut endoderm markers was maintained despite loss of *Foxa2* from ventral foregut endoderm (Fig. 6I–J). Markers utilized were *Foxa2* in presumptive floor plate, Brachyury in notochordal plate, and *Hlxb9* in notochord and dorsal foregut.

Aberrant ventral foregut morphogenesis in *Foxa2*<sup>loxP/loxP</sup>; *Isl1-Cre* mutants is associated with downregulation of epithelial and endodermal markers, decreased proliferation, and increased apoptosis in foregut endoderm

Ventral endoderm forms a highly organized epithelium with tight junctions. Recent studies have demonstrated a role for *Foxa2* in maintenance of epithelial integrity in the early embryo (Burtscher, 2009). Previous studies in mouse liver tissue have shown that *Foxa2* directly binds to regions within the *tight junction protein 1 (Tjp1)* locus encoding ZO-1 suggesting ZO-1 is a direct downstream target of *Foxa2* (Wederell et al., 2008). Therefore, we performed immunostaining for ZO-1 and ZO-2 in *Foxa2loxP/loxP*; *Isl1-Cre* embryos at 4–5 som. Apico-lateral localization of ZO-1 and ZO-2 was observed in epithelium of both formed and prospective foregut endoderm of control embryos (Fig. 7A). *Foxa2loxP/loxP*; *Isl1-Cre* endodermal segments composed of *Foxa2*-negative cells exhibited reduced to absent expression of both ZO-1 and ZO-2 (Fig. 7B). Isolated groups of *Foxa2*-expressing cells embedded in *Foxa2*-negative

epithelium displayed persistent expression of ZO-1 (data not shown) and ZO-2 (Fig. 7C,D), demonstrating that the observed effect is specific and cell autonomous.

To investigate whether *Foxa2* is required to maintain endodermal identity in foregut, immunohistochemistry was used to investigate expression of the transcription factor Sox17, a marker of endodermal identity (Kanai-Azuma et al., 2002). Control embryos with 4–5 som displayed several sites of specific positive signal for Sox17 in addition to foregut endoderm, including endocardium and cells throughout the mesenchyme that are often in close association with the foregut (Fig. 7E). Low levels of Sox17 expression reported in vascular and endocardial endothelium could account for some of the positive signal detected outside of the foregut (Sakamoto et al., 2007). Co-immunohistochemistry with an anti-E-cadherin antibody was performed to positively identify Sox17-expressing foregut endoderm. *Foxa2loxP/loxP*; *Isl1-Cre* embryos with 5 som displayed patches of E-cadherin-positive endoderm lacking Sox17 expression in the ventral foregut (Fig. 7E) that correlated with regions of reduced-to-absent *Foxa2* expression (data not shown). Sox17 expression was unchanged in dorsal foregut of mutant embryos.

Shortened foregut and defective midline cardiac fusion in *Foxa2loxP/loxP*; *Isl1-Cre* mutants indicated a role for *Foxa2* during ventral morphogenesis. Embryos homozygous null for the transcription factor *Gata4* similarly exhibit cardia bifida and lack of foregut closure (Kuo et al., 1997). Additionally, *Foxa2* directly binds to the *Gata4* locus in adult mouse liver, supporting a role for *Foxa2* as a direct upstream regulator of *Gata4* expression (Wederell et al., 2008). *Gata4* protein was detected in endoderm associated with cardiogenic mesoderm near the anterior intestinal portal of control embryos with 4–5 som (Fig. 7G). Endodermal *Gata4* expression was greatly reduced in this region of *Foxa2loxP/loxP*; *Isl1-Cre* mutants and correlated with areas of reduced-to-absent *Foxa2* protein levels (Fig. 7H,I).

To quantify shortened foregut pockets in *Foxa2loxP/loxP*; *Isl1-Cre* mutants, foregut pocket length was measured in 8.5 dpc

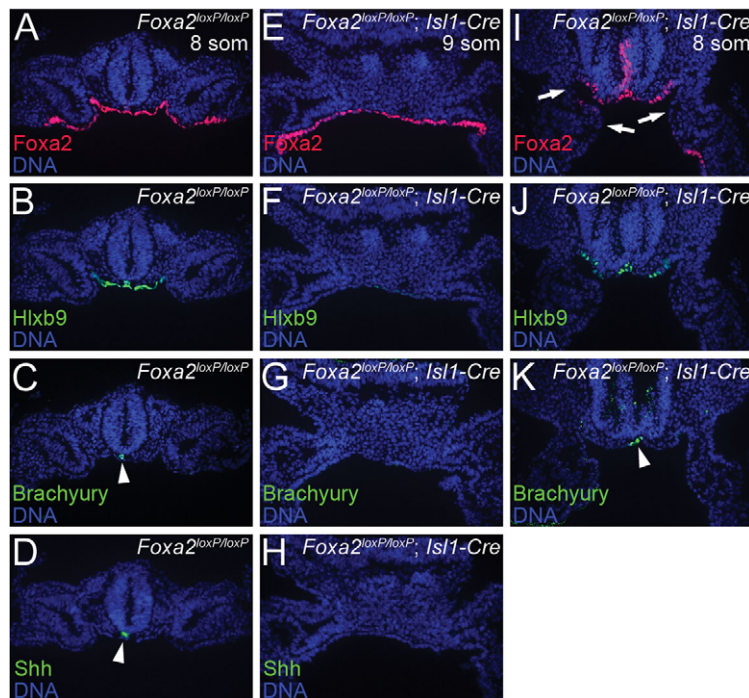


**Fig. 6. Lack of correlation between notochord marker expression in *Foxa2loxP/loxP*; *Isl1-Cre* embryos and *Foxa2* ablation in ventral foregut endoderm, 8.5 dpc.** Immunohistochemistry (IHC) to detect *Foxa2* (A, E, I), *Hlxb9* (B, F, J), Brachyury (C, G, K) and *Shh* (D, H) on transverse sections of *Foxa2loxP/loxP* (A–D) and *Foxa2loxP/loxP*; *Isl1-Cre* (E–H, I–K) embryos, 8–9 somite pairs (som). White arrowheads (C, D, K) indicate notochord as marked by Brachyury or *Shh* expression. The mutant in I–K maintained expression of axial tissue markers despite loss of *Foxa2* from ventral foregut endoderm (white arrows in I).

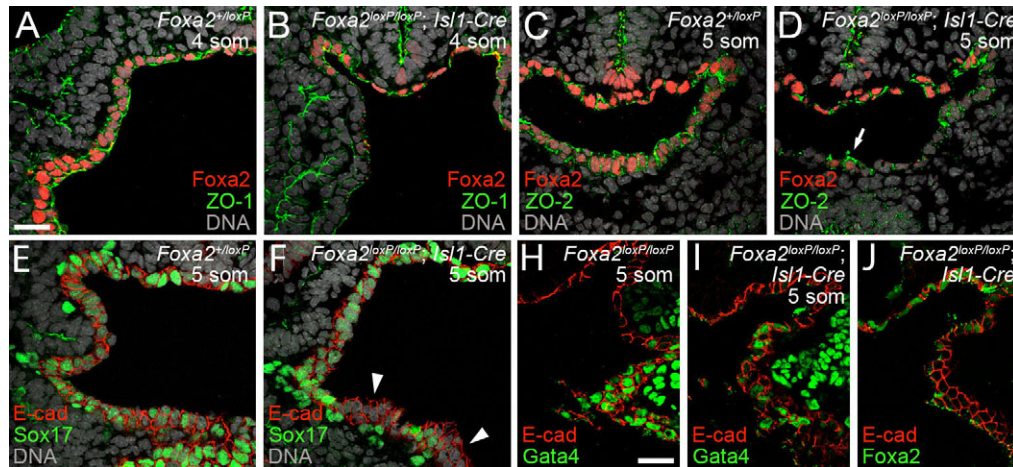


**Fig. 7. Decreased expression of proteins critical to ventral foregut morphogenesis in *Foxa2loxP/loxP*; *Isl1-Cre* embryos embryos.** (A–D) Anti-Foxa2 and anti-ZO-1 (A–B) or anti-ZO-2 (C–D) coimmunohistochemistry (IHC) on *Foxa2*<sup>+/loxP</sup> (A, C) and *Foxa2loxP/loxP*; *Isl1-Cre* (B, D) embryos with 4–5 somite pairs (som). (A–B) Sections posterior to the anterior intestinal portal. (C–D) Sections through the foregut. White arrow in D marks a cluster of cells retaining expression of both Foxa2 and ZO-2. (E–F) Sections of anti-SOX17, anti-E-cadherin co-IHC near the anterior intestinal portal of *Foxa2*<sup>+/loxP</sup> (E) and *Foxa2loxP/loxP*; *Isl1-Cre* (F) embryos with 5 som. Segments of ventral foregut endoderm lacking Sox17 expression were observed in the mutant (white arrowheads). (G–H) Anti-Gata4, anti-E-cadherin (E-cad) co-IHC on sections of *Foxa2loxP/loxP*; *Isl1-Cre* (G) and *Foxa2loxP/loxP*; *Isl1-Cre* (H) embryos with 5 somite pairs (som). Sections are posterior to the anterior intestinal portal. E-cadherin localizes to epithelial membranes and marks foregut endoderm. (I) Anti-Foxa2, anti-E-cadherin co-IHC on a section adjacent to that shown in B.

control and mutant embryos at 5 som. Analysis revealed that *Foxa2loxP/loxP*; *Isl1-Cre* mutants exhibited significantly shorter rostral-caudal foregut pocket length when compared to somite-matched controls (supplementary material Fig. S4).

To investigate potential causes for shortened foregut pocket length in mutants, foregut endoderm cell proliferation and apoptosis were compared between 8.5 dpc *Foxa2loxP/loxP*; *Isl1-Cre* and control embryos (4–6 som) (Fig. 8). To quantify proliferation, cells positive for the mitotic marker phosphohistone H3 (P-H3) were counted and calculated as a percentage of total foregut pocket cell number. Total foregut pocket P-H3 levels were significantly reduced in mutant versus control populations and correlated with significantly reduced proliferation in ventral foregut (Fig. 8 A–C). TUNEL assays were performed to assay apoptosis. TUNEL-positive cells were counted and calculated as a percentage of total foregut pocket cell number. Total foregut pocket TUNEL levels were significantly increased in mutant versus control populations and correlated with significantly increased levels in dorsal and ventral foregut (Fig. 8 D–F).

## Discussion

Embryological approaches in mouse have shown that prechordal plate is required to support identity and growth in overlying forebrain ectoderm (Shimamura and Rubenstein, 1997; Camus et al., 2000) with previous work suggesting involvement of *Foxa2* in these roles. Anterior embryo patterning phenotypes in mouse, such as holoprosencephaly, are correlated with disrupted expression of prechordal plate marker genes including *Foxa2* (Ang and Rossant, 1994; Weinstein et al., 1994; Filosa et al., 1997; Bachiller et al., 2000; Petryk et al., 2004; Nishioka et al., 2005; Warr et al., 2008). A role for *Foxa2* in prechordal plate during anterior embryo morphogenesis has also been supported by the phenotype of double *Gsc* null-*Foxa2* heterozygous mutants which exhibited abnormal forebrain morphology similar to that observed in *Foxa2loxP/loxP*; *Isl1-Cre* mutants (Filosa et al., 1997). Until now, genetic approaches to directly investigate patterning roles of prechordal plate, and roles for *Foxa2* in this tissue, have been encumbered by lack of a prechordal plate-specific Cre line that is exclusive of other axial mesendoderm components such as notochord. *Isl1Cre* ablates in

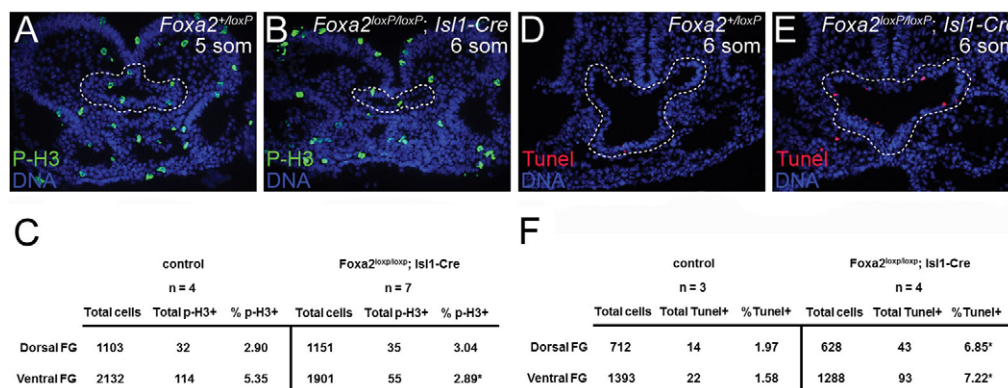


**Fig. 8. Proliferation and Apoptosis in Foregut of *Foxa2loxP/loxP*; *Isl1-Cre* Mutants.** (A, B) To assay proliferation, antibody to phosphorylated histone 3 (P-H3) was utilized on sections from somite matched littermate control or *Foxa2loxP/loxP*; *Isl1-Cre* mutants. (C) Quantitative analysis is shown. (D, E) Apoptosis was assessed by TUNEL staining of control or mutant sections. (F) Quantitative analysis is shown, demonstrating selective decrease in proliferation in ventral foregut, and increased apoptosis in both dorsal and ventral foregut. \* $P < 0.01$ .

prechordal plate and in ventral foregut endoderm, but not other axial mesendoderm. *Isl1-Cre*-mediated ablation of *Foxa2* results in anterior embryo patterning phenotypes previously seen consequent to perturbations of axial mesendoderm. These anterior patterning phenotypes were observed in mutant embryos which had preserved expression of *Foxa2* in ventral foregut endoderm. Conversely, notochord and dorsal foregut endoderm markers were present in embryos in which *Foxa2* was absent from ventral foregut endoderm. Taken together, our data suggest a primary role for *Foxa2* in prechordal plate for notochord development and/or maintenance. Ideally, it would be preferable to complement our studies with a Cre recombinase which would be selectively active in ventral foregut endoderm, and not in prechordal plate. However, our attempts to utilize *Nkx2.5cre* to this effect were unsuccessful, owing to perdurance of *Foxa2* protein in ventral foregut endoderm, despite successful recombination as indicated by lineage indicators.

Previous studies of dorsal foregut endoderm have focused on elucidating pathways that stimulate budding of organ primordia, such as pancreas (Zorn and Wells, 2009). Little is known as to factors which pattern dorsal foregut endoderm at earlier stages. *Foxa2<sup>loxP/loxP</sup>; Isl1-Cre* mutants exhibit reduced expression of the dorsal foregut marker *Hlxb9*. Lack of *Isl1-Cre* activity in dorsal foregut indicates a non-autonomous requirement for *Foxa2* in patterning of dorsal foregut endoderm. We observed a lack of correlation between loss of *Foxa2* in ventral foregut endoderm and downregulation of *Hlxb9*, suggesting a role for prechordal plate in maintenance of dorsal foregut endoderm identity. It is interesting to speculate that mutual signaling between contiguous dorsal endoderm and notochord may be required for specification or maintenance of both, and that this crosstalk may be disrupted in *Foxa2<sup>loxP/loxP</sup>; Isl1-Cre* mutants.

Previous work supports a model in which *Shh* secreted from axial mesendoderm induces *Foxa2* expression in overlying prospective floor plate; *Foxa2* in turn activates expression of *Shh* in this tissue. *Shh* secreted from floor plate is critical for dorsal-ventral neural patterning, such that homozygous null *Shh* mutants exhibit holoprosencephaly (Chiang et al., 1996; Sasaki et al., 1997; Ding et al., 1998; Matise et al., 1998; Epstein et al., 1999; Jeong and Epstein, 2003; Wilson and Maden, 2005). Floor plate secretes factors that function as a molecular boundary preventing asymmetric left-sided signaling networks from diffusing across the embryonic midline. Laterality phenotypes have been associated with disruption of this function in mice (Meno et al., 1998; Tsukui et al., 1999). Reduced or absent expression of *Shh* in the anterior embryo and *Foxa2* in neural groove indicated that this pathway was disrupted in *Foxa2<sup>loxP/loxP</sup>; Isl1-Cre* mutants which exhibited holoprosencephaly and laterality defects.

Surgical ablation of endodermal regions corresponding to prechordal plate in both chick and mouse models results in defective forebrain patterning, cardiac fusion, and foregut morphogenesis, supporting a role for prechordal plate in development of anterior-ventral tissues also affected in *Foxa2<sup>loxP/loxP</sup>; Isl1-Cre* mutants (Camus et al., 2000; Withington et al., 2001). Morphological abnormalities in *Foxa2<sup>loxP/loxP</sup>; Isl1-Cre* mutants also resemble what has been reported for Nodal loss-of-function mouse mutants in which defects have been attributed to deficient specification and/or formation of anterior axial mesendoderm populations, including prechordal plate (Roebroek et al., 1998; Lowe et al., 2001; Vincent et al., 2003; Dunn et al., 2004; Liu et al., 2004). While

*Shh* is required to promote survival within a subpopulation of cells comprising prechordal plate (Aoto et al., 2009), *Shh* null mutants exhibit heart and foregut developmental anomalies that occurred later and are less severe than those we have observed in *Foxa2<sup>loxP/loxP</sup>; Isl1-Cre* embryos (Litington et al., 1998; Smoak et al., 2005), identifying a *Shh*-independent *Foxa2*-mediated role for prechordal plate in ventral embryo morphogenesis.

We observed downregulation of a number of proteins which could, at least in part, account for observed defects in morphogenesis, proliferation, and survival of ventral endoderm in *Foxa2<sup>+/loxP</sup>; Isl1-Cre* mutants. *Isl1-Cre* mutants showed corresponding loss of *Foxa2* and *Gata4* expression in prospective ventral foregut endoderm cells near the site of closure. Homozygous null *Gata4* mutants exhibit ventral morphogenesis defects similar to those of *Foxa2<sup>+/loxP</sup>; Isl1-Cre* mutants, including cardiac bifida (Kuo et al., 1997; Molkenkin et al., 1997). Chimeric rescue experiments demonstrated a specific requirement for *Gata4* in endoderm for foregut closure (Kikugawa et al., 1997). Previous work showing that *Foxa2* directly binds to the *Gata4* locus support a role for *Foxa2* as a direct upstream regulator of *Gata4* expression (Wederell et al., 2008). Cardiac morphogenesis defects arising from ablation of *Foxa2* in prechordal plate and endoderm highlight an important caveat when using *Islet1Cre* to investigate the role of a gene in heart development. If the gene of interest overlaps with *Islet1Cre* in prechordal plate and/or ventral foregut endoderm, as well as the second heart field, any observed requirement for cardiogenesis consequent to ablation with *Islet1Cre* cannot be attributed to a requirement within the second heart field.

Foregut endoderm of *Foxa2loxP/loxP; Isl1-Cre* mutants also showed reduced expression of ZO-1 and ZO-2 tight junction scaffolding components. *Foxa2* has been shown to bind the *Tjp1* locus, encoding ZO-1, supporting a role for *Foxa2* as a direct upstream regulator of ZO-1 expression (Wederell et al., 2008). Homozygous ZO-1 null mutants die at 11.5 dpc, due to defects in yolk sac vascular development. Homozygous null ZO-2 mutants die at 9.5 dpc with disrupted tight junctions detected by 6.5–7.5 dpc. Both ZO-1 and ZO-2 null mutants displayed elevated levels of apoptosis throughout the embryo (Katsuno et al., 2008; Xu et al., 2008). In a mammary epithelial cell line, tight junction formation was only eliminated when both ZO-1 and ZO-2 function was downregulated, identifying a requirement the expression of both factors for tight junction assembly. Barrier function was compromised, although adherens-mediated cell adhesion appeared intact (Umeda et al., 2006; Umeda et al., 2004). The foregoing suggest that diminished expression of both ZO-1 and ZO-2 observed in the foregut of *Foxa2loxP/loxP; Isl1-Cre* embryos is likely to disrupt tight junction assembly and identifies a role for *Foxa2* in endoderm for maintenance of the foregut epithelium tight junction network. The *in vivo* requirement for ZO-1 and ZO-2 to prevent apoptosis suggests that loss of these factors in *Foxa2loxP/loxP; Isl1-Cre* embryos may contribute to increased cell death observed in mutant foregut.

## Materials and Methods

### Mouse lines, embryo collection

All mouse lines have been previously described: *Foxa2<sup>loxP</sup>* (Sund et al., 2000); *Isl1-Cre* (Yang et al., 2006); *Rosa<sup>26R-lacZ</sup>* (Soriano, 1999). *Foxa2<sup>loxP/loxP</sup>* or *Foxa2<sup>loxP/loxP</sup>; Rosa<sup>26R/26R</sup>* females were crossed with *Foxa2<sup>+/loxP</sup>; Isl1-Cre* males to generate embryos for morphological analysis, X-gal staining, *in situ* hybridization, immunohistochemistry. Matings were timed with noon on day of vaginal plug detection defined as 0.5 dpc.

$\beta$ -galactosidase staining, in situ hybridization, paraffin histology  
Embryos for whole-mount X-gal staining were collected between 7.5–10.5 dpc, fixed in 4% paraformaldehyde on ice 20–45 minutes depending on embryo size, stained according to described protocol (Nagy et al., 2003).

Embryos for in situ hybridization were collected between 8.0–8.5 dpc, fixed overnight at 4°C in 4% paraformaldehyde, dehydrated through a methanol series and stored in 100% methanol at –20°C. Whole-mount in situ hybridization was performed according to described protocol (Nagy et al., 2003) using the following probes: mouse *Brachyury*, *Fgf8*, *Foxa2*, *Gsc*, *Shh*. Samples were post-fixed overnight at 4°C in 4% paraformaldehyde. Post-fixed embryos processed for histology were embedded in paraffin wax and transverse sections cut at 8  $\mu$ m.

### Immunohistochemistry, TUNEL detection of apoptosis

Embryos for cryosectioning and immunohistochemistry were collected between 8.0–8.5 dpc, fixed in 4% paraformaldehyde on ice 20–30 minutes, washed twice in phosphate-buffered saline (PBS) containing 0.1% bovine serum albumin, and incubated through a PBS-sucrose series (5%, 12.5%, 20%). Incubations were performed on ice for 15–60 minutes each. Embryos were embedded in 1:1 mixture of 20% sucrose and Tissue-Tek O.C.T. Embedding Compound (Sakura Finetek). Sections were cut at 10  $\mu$ m unless otherwise noted.

Immunohistochemistry was performed according to described protocol (Nagy et al., 2003). 4',6-diamidino-2-phenylindole (DAPI, Invitrogen, D3571) was used to counterstain DNA. Primary antibodies used:  $\beta$ -galactosidase (1:400, MP Biomedicals, 56028); *Brachyury* (1:400, Santa Cruz Biotechnology, 17743); *Foxa2* (1:100, Santa Cruz Biotechnology, 6554); *Isl1* (1:1000, Abcam, 20670); phosphohistone H3 (1:200, Upstate Biotechnology, 06-570); *Shh* (1:150, Santa Cruz Biotechnology, 9024). Cleaved Caspase-3 (1:100, Cell Signaling Technology, cat. 9661); E-cadherin (1:300, Sigma-Aldrich, cat. U3254); *Gata4* (1:50, Santa Cruz Biotechnology, cat. 1237); *Hlx9* (1:8000, generously provided by Sam Pfaff, Salk Institute, La Jolla, CA); *SOX17* (1:300, R&D Systems, cat. AF1924); *ZO-1* (1:100, Invitrogen, cat. 40-2200); *ZO-2* (1:200, Invitrogen, cat. 71-1400). Secondary antibodies were from the Alexafluor series (Invitrogen Molecular Probes).

Sections for TUNEL-mediated detection of apoptosis were prepared as for immunohistochemistry and stained with *In Situ* Cell Death Detection Kit, TMR red according to manufacturer's instructions (Roche Applied Science, 12156792910).

### Acknowledgements

We thank the Evans lab, Carl de Luca, Michel Puceat, Ju Chen, Kunfu Ouyang and Deborah Yelon for helpful discussion and critical reading of the manuscript. We thank Maretoshi Hirai, Xingqun Liang, Jody Martin, David Stachura for technical guidance and Paul Chen for technical assistance. Probes provided by Richard Behringer, Bernhard Herrmann, Gail Martin, Deepak Srivastava, Kenneth Zaret. This work supported by NIH 5 R01 HL074066-03 (S.M.E.), NIH 1 F32 HL090291-01 (Z.H.), and AHA 0825280F (Z.H.).

### References

- Alexander, J., Rothenberg, M., Henry, G. L. and Stainier, D. Y. (1999). Casanova plays an early and essential role in endoderm formation in zebrafish. *Dev. Biol.* **215**, 343–357.
- Ang, S.-L. and Rossant, J. (1994). *HNF-3 $\beta$*  is essential for node and notochord formation in mouse development. *Cell* **78**, 561–574.
- Aoto, K., Shikata, Y., Imai, H., Matsumaru, D., Tokunaga, T., Shioda, S., Yamada, G. and Motoyama, J. (2009). Mouse *Shh* is required for prechordal plate maintenance during brain and craniofacial morphogenesis. *Dev. Biol.* **327**, 106–120.
- Bachiller, D., Klingensmith, J., Kemp, C., Belo, J. A., Anderson, R. M., May, S. R., McMahon, J. A., McMahon, A. P., Harland, R. M., Rossant, J. et al. (2000). The organizer factors Chordin and Noggin are required for mouse forebrain development. *Nature* **403**, 658–661.
- Beddington, R. S. P. (1994). Induction of a second neural axis by the mouse node. *Development* **120**, 613–620.
- Burtscher, L. H. (2009). *Foxa2* regulates polarity and epithelialization in the endoderm germ layer of the mouse embryo. *Development* **136**, 1029–1038.
- Camus, A., Davidson, B. P., Billiards, S., Khoo, P.-L., Rivera-Pérez, J. A., Wakamiya, M., Behringer, R. R. and Tam, P. P. L. (2000). The morphogenetic role of midline mesoderm and ectoderm in the development of the forebrain and the midbrain of the mouse embryo. *Development* **127**, 1799–1813.
- Chiang, C., Litingtung, Y., Lee, E., Young, K. E., Corden, J. L., Westphal, H. and Beachy, P. A. (1996). Cyclopia and defective axial patterning in mice lacking *Sonic hedgehog* gene function. *Nature* **383**, 407–413.
- Couly, G. F., Coltey, P. M. and Le Douarin, N. M. (1992). The developmental fate of the cephalic mesoderm in quail-chick chimeras. *Development* **114**, 1–15.
- Crossley, P. H. and Martin, G. R. (1995). The mouse *Fgf8* gene encodes a family of polypeptides and is expressed in regions that direct outgrowth and patterning in the developing embryo. *Development* **121**, 439–451.
- Ding, Q., Motoyama, J., Gasca, S., Mo, R., Sasaki, H., Rossant, J. and Hui, C. (1998). Diminished *Sonic hedgehog* signaling and lack of floor plate differentiation in *Gli2* mutant mice. *Development* **125**, 2533–2543.
- Dufort, D., Schwartz, L., Harpal, K. and Rossant, J. (1998). The transcription factor *HNF3 $\beta$*  is required in visceral endoderm for normal primitive streak morphogenesis. *Development* **125**, 3015–3025.
- Dunn, N. R., Vincent, S. D., Oxburgh, L., Robertson, E. J. and Bikoff, E. K. (2004). Combinatorial activities of *Smad2* and *Smad3* regulate mesoderm formation and patterning in the mouse embryo. *Development* **131**, 1717–1728.
- Echelard, Y., Epstein, D. J., St-Jacques, B., Shen, L., Mohler, J., McMahon, J. A. and McMahon, A. P. (1993). *Sonic hedgehog*, a member of a family of putative signaling molecules, is implicated in the regulation of CNS polarity. *Cell* **75**, 1417–1430.
- Epstein, D. J., McMahon, A. P. and Joyner, A. L. (1999). Regionalization of *Sonic hedgehog* transcription along the anteroposterior axis of the mouse central nervous system is regulated by *Hnf3*-dependent and -independent mechanisms. *Development* **126**, 281–292.
- Filosa, S., Rivera-Pérez, J. A., Gómez, A. P., Gansmuller, A., Sasaki, H., Behringer, R. R. and Ang, S.-L. (1997). *Goosecoid* and *HNF-3 $\beta$*  genetically interact to regulate neural tube patterning during mouse embryogenesis. *Development* **124**, 2843–2854.
- Franklin, V., Khoo, P. L., Bildsoe, H., Wong, N., Lewis, S. and Tam, P. P. L. (2008). Regionalisation of the endoderm progenitors and morphogenesis of the gut portals of the mouse embryo. *Mech. Dev.* **125**, 587–600.
- Jeong, Y. and Epstein, D. J. (2003). Distinct regulators of *Shh* transcription in the floor plate and notochord indicate separate origins for these tissues in the mouse node. *Development* **130**, 3891–3902.
- Jessell, T. M. (2000). Neuronal specification in the spinal cord: inductive signals and transcriptional codes. *Nat. Rev. Genet.* **1**, 20–29.
- Jurand, A. (1974). Some aspects of the development of the notochord in mouse embryos. *J. Embryol. Exp. Morphol.* **32**, 1–33.
- Kanai-Azuma, M., Kanai, Y., Gad, J. M., Tajima, Y., Taya, C., Kurohmaru, M., Sanai, Y., Yonekawa, H., Yazaki, K., Tam, P. P. et al. (2002). Depletion of definitive gut endoderm in *Sox17*-null mutant mice. *Development* **129**, 2367–2379.
- Katsuno, T., Umeda, K., Matsui, T., Hata, M., Tamura, A., Itoh, M., Takeuchi, K., Fujimori, T., Nabeshima, Y., Noda, T. et al. (2008). Deficiency of zonula occludens-1 causes embryonic lethal phenotype associated with defected yolk sac angiogenesis and apoptosis of embryonic cells. *Mol. Biol. Cell* **19**, 2465–2475.
- Kikugawa, K. N. R., Inuzuka, T., Kokubo, Y., Narita, Y., Kuzuhara, S., Yoshida, S. and Tsuji, S. (1997). A missense mutation in the *SOD1* gene in patients with amyotrophic lateral sclerosis from the Kii Peninsula and its vicinity, Japan. *Neurogenetics* **1**, 113–115.
- Kinder, S. J., Tsang, T. E., Wakamiya, M., Sasaki, H., Behringer, R. R., Nagy, A. and Tam, P. P. L. (2001). The organizer of the mouse gastrula is composed of a dynamic population of progenitor cells for the axial mesoderm. *Development* **128**, 3623–3634.
- Kirby, M. L., Lawson, A., Stadt, H. A., Kumiski, D. H., Wallis, K. T., McCraney, E., Waldo, K. L., Li, Y.-X. and Schoenwolf, G. C. (2003). Hensen's node gives rise to the ventral midline of the foregut: implications for organizing head and heart development. *Dev. Biol.* **253**, 175–188.
- Kuo, C. T., Morrisey, E. E., Anandappa, R., Sigrist, K., Lu, M. M., Parmacek, M. S., Soudais, C. and Leiden, J. M. (1997). *GATA4* transcription factor is required for ventral morphogenesis and heart tube formation. *Genes Dev.* **11**, 1048–1060.
- Lee, C. S., Sund, N. J., Behr, R., Herrera, P. L. and Kaestner, K. H. (2005). *Foxa2* is required for the differentiation of pancreatic  $\alpha$ -cells. *Dev. Biol.* **278**, 484–495.
- Lee, J. D. and Anderson, K. V. (2008). Morphogenesis of the node and notochord: the cellular basis for the establishment and maintenance of left-right asymmetry in the mouse. *Dev. Dyn.* **237**, 3464–3476.
- Lewis, S. L. and Tam, P. P. L. (2006). Definitive endoderm of the mouse embryo: formation, cell fates, and morphogenetic function. *Dev. Dyn.* **235**, 2315–2329.
- Litingtung, Y., Lei, L., Westphal, H. and Chiang, C. (1998). *Sonic hedgehog* is essential to foregut development. *Nat. Genet.* **20**, 58–61.
- Liu, Y., Festing, M., Thompson, J. C., Hester, M., Rankin, S., El-Hodiri, H. M., Zorn, A. M. and Weinstein, M. (2004). *Smad2* and *Smad3* coordinately regulate craniofacial and endodermal development. *Dev. Biol.* **270**, 411–426.
- Lowe, L. A., Yamada, S. and Kuehn, M. R. (2001). Genetic dissection of *nodal* function in patterning the mouse embryo. *Development* **128**, 1831–1843.
- Maretto, S., Müller, P. S., Aricescu, A. R., Cho, K. W., Bikoff, E. K. and Robertson, E. J. (2008). Ventral closure, headfold fusion and definitive endoderm migration defects in mouse embryos lacking the fibronectin leucine-rich transmembrane protein FLRT3. *Dev. Biol.* **318**, 184–193.
- Matise, M. P., Epstein, D. J., Park, H. L., Platt, K. A. and Joyner, A. L. (1998). *Gli2* is required for induction of floor plate and adjacent cells, but not most ventral neurons in the mouse central nervous system. *Development* **125**, 2759–2770.
- Meno, C., Shimono, A., Sajoh, Y., Yashiro, K., Mochida, K., Ohishi, S., Noji, S., Kondoh, H. and Hamada, H. (1998). *Lefty-1* is required for left-right determination as a regulator of *lefty-2* and *nodal*. *Cell* **94**, 287–297.
- Molkentin, J. D., Lin, Q., Duncan, S. A. and Olson, E. N. (1997). Requirement of the transcription factor *GATA4* for heart tube formation and ventral morphogenesis. *Genes Dev.* **11**, 1061–1072.
- Muenke, M. and Beachy, P. A. (2000). Genetics of ventral forebrain development and holoprosencephaly. *Curr. Opin. Genet. Dev.* **10**, 262–269.
- Nagy, A., Gertenstein, M., Vintersten, K. and Behringer, R. (2003). In *Manipulating the Mouse Embryo, A Laboratory Manual, Third Edition* (ed J. Inglis, J. Cuddihy, M.

- Cozza, P. Barker, D. deBruin, D. Weiss and E. Atkeson), pp. 629-706. Cold Spring Harbor, NY: Cold Spring Harbor Laboratory Press.
- Nishioka, N., Nagano, S., Nakayama, R., Kiyonari, H., Ijiri, T., Taniguchi, K., Shawlot, W., Hayashizaki, Y., Westphal, H., Behringer, R. R. et al. (2005). Ssd1 regulates head morphogenesis of mouse embryos by activating the Lim1-Ldb1 complex. *Development* **132**, 2535-2546.
- Park, E. J., Ogdan, L. A., Talbot, A., Evans, S., Cai, C. L., Black, B. L., Frank, D. U. and Moon, A. M. (2006). Required, tissue-specific roles for Fgf8 in outflow tract formation and remodeling. *Development* **133**, 2419-2433.
- Petryk, A., Anderson, R. M., Jarcho, M. P., Leaf, I., Carlson, C. S., Klingensmith, J., Shawlot, W. and O'Connor, M. B. (2004). The mammalian twisted gastrulation gene functions in foregut and craniofacial development. *Dev. Biol.* **267**, 374-386.
- Roebroek, A. J. M., Umans, L., Pauli, I. G. L., Robertson, E. J., van Leuven, F., Van de Ven, W. J. M. and Constam, D. B. (1998). Failure of ventral closure and axial rotation in embryos lacking the proprotein convertase Furin. *Development* **125**, 4863-4876.
- Sakamoto, Y., Hara, K., Kanai-Azuma, M., Matsui, T., Miura, Y., Tsunekawa, N., Kurohmaru, M., Saijoh, Y., Koopman, P. and Kanai, Y. (2007). Redundant roles of Sox17 and Sox18 in early cardiovascular development of mouse embryos. *Biochem. Biophys. Res. Commun.* **360**, 539-544.
- Sasaki, H., Hui, C., Nakafuku, M. and Kondoh, H. (1997). A binding site for Gli proteins is essential for *HNF-3 $\beta$*  floor plate enhancer activity in transgenics and can respond to Shh in vitro. *Development* **124**, 1313-1322.
- Shimamura, K. and Rubenstein, J. L. R. (1997). Inductive interactions direct early regionalization of the mouse forebrain. *Development* **124**, 2709-2718.
- Smoak, I. W., Byrd, N. A., Abu-Issa, R., Goddeeris, M. M., Anderson, R., Morris, J., Yamamura, K., Klingensmith, J. and Meyers, E. N. (2005). *Sonic hedgehog* is required for cardiac outflow tract and neural crest cell development. *Dev. Biol.* **283**, 357-372.
- Soriano, P. (1999). Generalized *lacZ* expression with the ROSA26 Cre reporter strain. *Nat. Genet.* **21**, 70-71.
- Sulik, K., Dehart, D. B., Iangaki, T., Carson, J. L., Vrablic, T., Gesteland, K. and Schoenwolf, G. C. (1994). Morphogenesis of the murine node and notochordal plate. *Dev. Dyn.* **201**, 260-278.
- Sund, N. J., Ang, S.-L., Sackett, S. D., Shen, W., Daigle, N., Magnuson, M. A. and Kaestner, K. H. (2000). Hepatocyte nuclear factor 3 $\beta$  (*foxa2*) is dispensable for maintaining the differentiated state of the adult hepatocyte. *Mol. Cell. Biol.* **20**, 5175-5183.
- Tam, P. P. L., Khoo, P.-L., Lewis, S. L., Bildsoe, H., Wong, N., Tsang, T. E., Gad, J. M. and Robb, L. (2007). Sequential allocation and global pattern of movement of the definitive endoderm in the mouse embryo during gastrulation. *Development* **134**, 251-260.
- Tremblay, K. D. and Zaret, K. S. (2005). Distinct populations of endoderm cells converge to generate the embryonic liver bud and ventral foregut tissues. *Dev. Biol.* **280**, 87-99.
- Tsukui, T., Capdevila, J., Tamura, K., Ruiz-Lozano, P., Rodriguez-Esteban, C., Yonei-Tamura, S., Magallón, J., Chandraratna, R. A. S., Chien, K., Blumberg, B. et al. (1999). Multiple left-right asymmetry defects in *Shh*<sup>-/-</sup> mutant mice unveil a convergence of the Shh and retinoic acid pathways in the control of *Lefty-1*. *Proc. Natl. Acad. Sci. USA* **96**, 11376-11381.
- Tzahor, E. and Evans, S. M. (2011). Pharyngeal mesoderm development during embryogenesis: implications for both heart and head myogenesis. *Cardiovasc. Res.* **91**, 196-202.
- Umeda, K., Matsui, T., Nakayama, M., Furuse, K., Sasaki, H., Furuse, M. and Tsukita, S. (2004). Establishment and characterization of cultured epithelial cells lacking expression of ZO-1. *J. Biol. Chem.* **279**, 44785-44794.
- Umeda, K., Ikenouchi, J., Katahira-Tayama, S., Furuse, K., Sasaki, H., Nakayama, M., Matsui, T., Tsukita, S., Furuse, M. and Tsukita, S. (2006). ZO-1 and ZO-2 independently determine where claudins are polymerized in tight-junction strand formation. *Cell* **126**, 741-754.
- Vincent, S. D., Dunn, N. R., Hayashi, S., Norris, D. P. and Robertson, E. J. (2003). Cell fate decisions within the mouse organizer are governed by graded Nodal signals. *Genes Dev.* **17**, 1646-1662.
- Warr, N., Powles-Glover, N., Chappell, A., Robson, J., Norris, D. and Arkell, R. M. (2008). *Zic2*-associated holoprosencephaly is caused by a transient defect in the organizer region during gastrulation. *Hum. Mol. Genet.* **17**, 2986-2996.
- Wederell, E. D., Bilenky, M., Cullum, R., Thiessen, N., Dagninar, M., Delaney, A., Varhol, R., Zhao, Y., Zeng, T., Bernier, B. et al. (2008). Global analysis of in vivo Foxa2-binding sites in mouse adult liver using massively parallel sequencing. *Nucleic Acids Res.* **36**, 4549-4564.
- Weinstein, D. C., Ruiz i Altaba, A., Chen, W. S., Hoodless, P., Prezioso, V. R., Jessell, T. M. and Darnell, J. E., Jr. (1994). The winged-helix transcription factor *HNF-3 $\beta$*  is required for notochord development in the mouse embryo. *Cell* **78**, 575-588.
- Wilson, L. and Maden, M. (2005). The mechanisms of dorsoventral patterning in the vertebrate neural tube. *Dev. Biol.* **282**, 1-13.
- Withington, S., Beddington, R. and Cooke, J. (2001). Foregut endoderm is required at head process stages for anteriormost neural patterning in chick. *Development* **128**, 309-320.
- Xu, J., Kausalya, P. J., Phua, D. C. Y., Ali, S. M., Hossain, Z. and Hunziker, W. (2008). Early embryonic lethality of mice lacking ZO-2, but Not ZO-3, reveals critical and nonredundant roles for individual zonula occludens proteins in mammalian development. *Mol. Cell. Biol.* **28**, 1669-1678.
- Yamanaka, Y., Tamplin, O. J., Beckers, A., Gossler, A. and Rossant, J. (2007). Live Imaging and Genetic Analysis of Mouse Notochord Formation Reveals Regional Morphogenetic Mechanisms. *Dev. Cell* **13**, 884-896.
- Yang, L., Cai, C.-L., Lin, L., Qyang, Y., Chung, C., Monteiro, R. M., Mummery, C. L., Fishman, G. I., Cogen, A. and Evans, S. (2006). Isl1Cre reveals a common Bmp pathway in heart and limb development. *Development* **133**, 1575-1585.
- Yuan, S. and Schoenwolf, G. (2000). Islet-1 marks the early heart rudiments and is asymmetrically expressed during early rotation of the foregut in the chick embryo. *Anat. Rec.* **260**, 204-207.
- Zorn, A. M. and Wells, J. M. (2009). Vertebrate endoderm development and organ formation. *Annu. Rev. Cell Dev. Biol.* **25**, 221-251.